Extension of core polarization in inelastic scattering to include charge-exchange reactions

V. R. Brown*
Lawrence Livermore Laboratory, University of California, Livermore, California 94550

V. A. Madsen*†
Oregon State University, Corvallis, Oregon 97331
(Received 27 December 1977)

An earlier formulation rougly relating core-polarization effects for different external fields, electromagnetic (p,p'), (α,α'), etc., through a 2×2 core-polarization matrix has been generalized to include charge-exchange reactions under the assumption that the isospin of the nuclear states is pure. The pure isovector field of the direct charge-exchange reaction to an excited-analog state has both an isovector and an *isoscalar* field for the model space as in inelastic scattering. A crude schematic representation of the giant resonances, virtually excited by interaction with the model space and responsible for the core polarization, is used to estimate the effect on the core-polarization parameters of imposing isospin conservation. The results of the earlier formulation are changed only slightly. Direct excitation of giant-quadrupole resonances in ^{208}Pb by (p,p') and (n,p) are compared. Energy shifts of the $T_>$ and $T_<$ isovector giant-quadrupole resonances are compared with the corresponding dipole shifts.

[NUCLEAR REACTIONS Low lying $0^+ \rightarrow 2^+$ transitions; extension of core-polarization effects to include charge exchange by application of isospin conservation. Giant-quadrupole transition rates and isovector splitting estimated.]

I. INTRODUCTION

In a recent paper[1] we have shown that the concept of effective charges for nuclear transitions in neutron-excess nuclei must be generalized when one considers various external fields such as the electromagnetic interaction, (α,α'), (p,p'), etc. This need is due to the fact that in nuclei with a neutron excess the giant-resonance states, thought to be largely responsible for the polarization charge, are expected to depart from a purely isovector or isoscalar character. As a result the usual effective nuclear transition operator

$$a_0 + a_1 \tau_z \tag{1}$$

gets replaced by

$$a_0^{\text{eff}} + a_1^{\text{eff}} \tau_z' . \tag{2}$$

The operator τ_z' operates only on model-space nucleons, and the coefficients a_τ^{eff} are given by the relation

$$\begin{pmatrix} a_0^{\text{eff}} \\ a_1^{\text{eff}} \end{pmatrix} = \underline{\epsilon} \begin{pmatrix} a_0 \\ a_1 \end{pmatrix} . \tag{3}$$

In Eq. (3) $\underline{\epsilon}$ is a 2×2 matrix which is expected to be nondiagonal in $N \neq Z$ nuclei. In the limit of pure isoscalar and isovector giant-resonance states or in nuclei with $N=Z$, $\epsilon_{01}=\epsilon_{10}=0$, $\epsilon_{00}=e_0$, and $\epsilon_{11}=e_1$, the isoscalar and isovector effective charges.

The main aim of this paper is to extend the results of Ref. 1 to charge-exchange reactions. Among other results we show how the ϵ matrix can be used for charge-exchange reactions when the conservation of isospin is taken into account. The main results of Ref. 1 are unchanged by this improvement.

II. CORE POLARIZATION IN INELASTIC SCATTERING

We make up a giant-resonance state of a nucleus by coupling particle-hole pairs with the nuclear model space. It is convenient to classify the particle-hole pairs as matched (ma) or unmatched (un) types as in Fig. 1, according to whether the neutron and proton particle-hole pairs can occupy the same or only different orbits, respectively. In the idealization that the nucleus consists of filled independent-particle states, the unmatched type pairs give states of definite isospin,[2] $T=T_0=(N-Z)/2$. The matched type can produce states of $T=T_0$ and $T=T_0\pm 1$. Our Tamm-Dancoff approximation (TDA) giant states can be written as follows

$$|\hbar\omega_{T_0}; T_0, T_0\rangle = \left(\sum_{mi}^{\text{un}} C_{mi}^{n}\, a_{m1/2}^{\dagger} b_{i-1/2}^{\dagger} + \sum_{mi}^{\text{un}} C_{mi}^{p}\, a_{m-1/2}^{\dagger} b_{i1/2}^{\dagger} \right)_{\lambda\mu} |T_0, T_0\rangle + \sum_{\tau} \sum_{mi}^{\text{ma}} B_{mi}^{\tau} [[a_m^{\dagger} b_i^{\dagger}]_{\lambda\mu\tau} |T_0\rangle]_{T_0 T_0} \tag{4a}$$

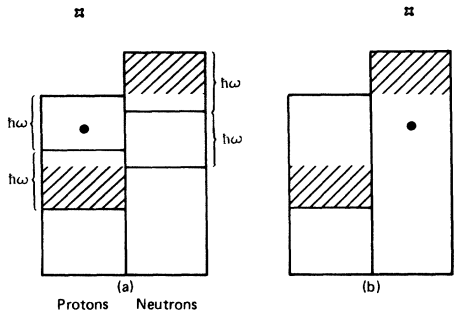

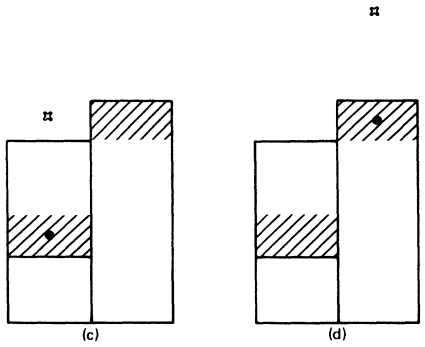

FIG. 1. Types of particle-hole excitations. Figures 1(a) and 1(b) are matched types, linear combinations of which can be taken to be purely isovector or isoscalar. These are then coupled to the ground state of the nucleus with isospin T_0 to form excitations with $T = T_0$ or $T_0 + 1$. Figure 1(c) has no corresponding neutron particle-hole and Fig. 1(d) has no corresponding proton particle-hole pair, so each of them are completely mixed in isospin. When coupled with the nuclear ground state of T_0 they each produce only $T = T_0$ pieces. The quadrupole transitions particle-hole pairs come primarily from $2\hbar\omega$ below to the top of the Fermi sea. The shaded areas represent sources of unmatched neutron and proton particle-hole pairs, and the space between is the source of matched particle-hole pairs.

for $T = T_0$, and

$$|\hbar\omega_T; T, T_Z\rangle = \sum_{mi}^{ma} B^1_{mi} [[a^\dagger_m b^\dagger_i]_{\lambda\mu 1} |T_0\rangle]_{TT_Z} \qquad (4b)$$

for $T \neq T_0$. Note that the coupling of the matched-type particle-hole pairs to the T_0 ground state in Eq. (4a) includes components with $\tau_z = 0$, $T_z = T_0$ and $\tau_z = 1$, $T_z = T_0 - 1$. The latter is built on an analog state in the model space and diagramatically would be represented[2] by Fig. 2 as a two-particle, two-hole state.

The polarization will now be calculated using the diagrams in Figs. 1 and 2 to represent the polarization terms in both the initial and final states in some nuclear transition. We ignore differences in the particle-hole excitations due to different blocking effects in the initial or final model states. The model-space wave functions are perturbed by their interaction with the particle-hole pairs:

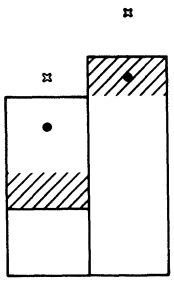

FIG. 2. A diagram representing a component needed for a good-isospin wave function with a charge-exchanged core and particle-hole pair.

$$\psi_i = \psi^0_i - \sum_t \frac{\langle [A^\dagger_t \psi^0_f]_i | V | \psi^0_i \rangle [A^\dagger_t \psi^0_f]_i}{E_t + E_f - E_i} , \qquad (5a)$$

$$\psi_f = \psi^0_f - \sum_t \frac{\langle [A^\dagger_t \psi^0_i]_f | V | \psi^0_f \rangle [A^\dagger_t \psi^0_i]_f}{E_t + E_i - E_f} , \qquad (5b)$$

where $A^\dagger_t$ is an operator which produces the particle-hole giant-resonance excitation built on the model state. We consider two cases: (1) $T_i = T_f = T_0$: In this case $[A^\dagger_t \psi^0_f]_i$ and $[A^\dagger_t \psi^0_i]_f$ represent $T = T_0$ giant resonances built on the final and initial states. (2) $T_i = T_0$, $T_f = T_0 + 1$: In this case $[A^\dagger_t \psi^0_f]_i$ represents a $T = T_0$ giant resonance built on a $T = T_0 + 1$ state, and $[A^\dagger_t \psi^0_i]_f$ represents a $T = T_0 + 1$ ($T_>$) giant resonance built on the T_0 ground state. There is no need to consider separately charge exchange to analog states in the $T_z = T_0 - 1$ neighboring nucleus or to $T = T_0 + 1$ states in the $T_z = T_0 \pm 1$ nucleus since these are related by Clebsch-Gordan coefficients to the analogous inelastic-scattering transitions.

As in Ref. 1 we now calculate the matrix element between states represented by Eqs. (5a) and (5b) of some multipole operator

$$\sum_\tau a_\tau \mathcal{O}_{\lambda\mu\tau\rho} = \sum_{i=1}^{A} \mathcal{O}_{\lambda\mu}(i)[a_0 + a_1 \tau_\rho(i)] \qquad (6)$$

representing the effects on the nuclear coordinates of an external field such as electromagnetic, (p,p'), (n,n'), (p,n), etc. In Eq. (6) τ_ρ is the ρ component of the single-particle isospin operator τ. (Obviously if $\rho \neq 0$, $a_0 = 0$.)

The matrix element to first order is

$$\langle\psi_f|\mathcal{O}_{\lambda\mu\tau\rho}|\psi_i\rangle=\langle\psi_f^0|\mathcal{O}_{\lambda\mu\tau\rho}|\psi_i^0\rangle-\sum_t\frac{\langle\psi_f^0|\mathcal{O}_{\lambda\mu\tau\rho}|[A_t^\dagger\psi_f^0]_i\rangle\langle[A_t^\dagger\psi_f^0]_i|V|\psi_i^0\rangle}{E_t+E_f-E_i}$$
$$-\sum_t\frac{\langle[A_t^\dagger\psi_i^0]_f|\mathcal{O}_{\lambda\mu\tau\rho}|\psi_i^0\rangle\langle\psi_f^0|V|[A_t^\dagger\psi_i^0]_f\rangle}{E_t+E_i-E_f}. \tag{7}$$

A. Case (1), $T_i=T_f=T_0$

As in Ref. 1, a separable central interaction,

$$V=\sum V_\tau\underline{\mathcal{O}}_{\lambda\tau}(\text{model})\cdot\underline{\mathcal{O}}_{\lambda\tau}(\text{ph}), \tag{8}$$

is used. The giant-resonance excitation of isospin T_0 built on a model-space wave function ψ of isospin T_0 with projection T_0 can be written

$$[A_t^\dagger\psi^0]_{JT_0}\equiv[A_t^{\text{un}\dagger}\psi^0]_J+[A_t^{0\dagger}\psi^0]_J+[A_t^{1\dagger}\psi^0]_{JT_0}, \tag{9}$$

where $[A_t^{\text{un}\dagger}\psi^0]_J$ is the unmatched and $[A_t^\dagger\psi^0]_{JT_0}$ a matched part of Eq. (4). Note that we have explicitly excluded a $T_>=T_0+1$ component which would violate the purity of isospin assumed for the perturbed wave functions of Eqs. (5). The λ multipole of the potential matrix element of the third term in Eq. (7) is

$$\langle\psi_f^0|V|[A_t^\dagger\psi_i^0]_f\rangle=\sum_\tau V_\tau\langle\psi_f^0|\underline{\mathcal{O}}_{\lambda\tau}(\text{model})\cdot\underline{\mathcal{O}}_{\lambda\tau}(\text{ph})|[(A_t^{\text{un}}+A_t^0+A_t^1)^\dagger\psi_i^0]_f\rangle$$
$$=\sum_\tau V_\tau\langle J_i\lambda M_i\mu|J_fM_f\rangle^{-1}\left[S_\tau^t(\text{un})+\delta_{\tau0}S_0^t(\text{ma})+\delta_{\tau1}\left(\frac{T_0+1}{T_0}\right)^{1/2}S_1^t(\text{ma})\right]\langle\psi_{J_fT_0}^0|\mathcal{O}_{\lambda\mu\tau0}|\psi_{J_iT_0}^0\rangle, \tag{10}$$

where, in terms of the particle-hole (ph) vacuum, the transition strengths are

$$S_\tau^t(\text{un})=\langle A_{t\lambda\mu}^{\text{un}\dagger}\psi_{\text{vac}}|\mathcal{O}_{\lambda\mu\tau0}|\psi_{\text{vac}}\rangle,$$
$$S_\tau^t(\text{ma})=\langle A_{t\lambda\mu}^{\text{ma}\dagger}\psi_{\text{vac}}|\mathcal{O}_{\lambda\mu\tau0}|\psi_{\text{vac}}\rangle, \tag{11}$$

and the operator matrix element of the third term of Eq. (7) is

$$\langle[A_t^\dagger\psi_i^0]_f|\mathcal{O}_{\lambda\mu\tau0}|\psi_i^0\rangle=\langle J_i\lambda M_i\mu|J_fM_f\rangle$$
$$\times\left[S_\tau^t(\text{un})+\delta_{\tau0}S_0^t(\text{ma})+\delta_{\tau1}\left(\frac{T_0}{T_0+1}\right)^{1/2}S_1^t(\text{ma})\right]. \tag{12}$$

The reduction of the isovector transition strength due to the exclusion of the $T_>=T_0+1$ excitation is expressed by the factor $[T_0/(T_0+1)]^{1/2}$ in the third term in the brackets of Eq. (12). A similar reduction in the matrix element of Eq. (10) is more than compensated by the inclusion of charge-exchange parts of the $\vec{\tau}\cdot\vec{\tau}$ operator, in the valence-core interaction.

For $E_t^2\gg(E_f-E_i)^2$ the second and third terms of Eq. (7) are combined using Eqs. (10) and (12) to give a result analogous to Ref. 1,

$$\langle\psi_f|\sum_\tau a_\tau\mathcal{O}_{\lambda\mu\tau0}|\psi_i\rangle=\langle\psi_f^0|\sum_{\tau'}a_{\tau'}^{\text{eff}}\mathcal{O}_{\lambda\mu\tau'0}|\psi_i^0\rangle, \tag{13}$$

where

$$a_\tau^{\text{eff}}=\sum_\tau\epsilon_{\tau'\tau}a_\tau. \tag{14}$$

This is equivalent to Eq. (3) with

$$\underline{\epsilon}=\underline{1}-2\underline{V}\underline{\sigma}, \tag{15}$$

$$V_{\tau'\tau}=\delta_{\tau'\tau}V_\tau, \tag{16a}$$

$$\sigma_{\tau'\tau}=\sum_t\frac{\bar{S}_{\tau'}^tS_\tau^t}{E_t}, \tag{16b}$$

and

$$S_\tau^t=S_\tau^t(\text{un})+\delta_{\tau0}S_0^t(\text{ma})+\delta_{\tau1}\left(\frac{T_0}{T_0+1}\right)^{1/2}S_1^t(\text{ma}), \tag{17a}$$

$$\bar{S}_{\tau'}^t=S_{\tau'}^t(\text{un})+\delta_{\tau'0}S_0^t(\text{ma})+\delta_{\tau'1}\left(\frac{T_0+1}{T_0}\right)^{1/2}S_1^t(\text{ma}). \tag{17b}$$

The only essential difference in these results and those of Ref. 1 is the asymmetry of the σ matrix, and according to Eq. (17) this difference vanishes in the limit of large neutron excess. This is due to the fact that the $T_>$ part of the isovector excitation has a vanishing inelastic excitation strength in the limit of large neutron excess.

B. Case (2), $T_f=T_o+1$

Since only the $\tau=1$ transfer is possible in these cases, the $\underline{\epsilon}$ matrix is 1×1, so the multipole matrix element is

$$\langle \psi_{fT} | \mathcal{O}_{\lambda\mu 1\rho} | \psi_{iT_0} \rangle \approx \langle \psi^0_{fT} | \mathcal{O}_{\lambda\mu 1\rho} | \psi^0_{iT_0} \rangle \left(1 - \frac{2V_1}{E_t} |S^t_1(\mathrm{ma})|^2\right), \quad (18)$$

where again it is assumed that $E_t^2 \gg (E_f - E_i)^2$. This may not be the case for $T_> = T_0 + 1$ states, so $2/E_t$ must be replaced by $2E_t/[E_t^2 - (E_f - E_i)^2]$. Equation (18) implies that transitions to $T_>$ states below the $T_>$ giant resonance are retarded.

C. Core polarization in excited-analog transitions

Since the perturbed wave functions, Eqs. (5) have definite isospin, the inelastic scattering and charge-exchange transitions are analogous. Therefore, the effective operators have the same relation to the bare operators in charge exchange as in inelastic scattering. Since in charge exchange, the bare operator includes only a $\tau = 1$ part, the effective operator has strength parameters

$$\begin{pmatrix} a_0^{\mathrm{eff}} \\ a_0^{\mathrm{eff}} \end{pmatrix} = \begin{pmatrix} \epsilon_{00} & \epsilon_{01} \\ \epsilon_{10} & \epsilon_{11} \end{pmatrix} \begin{pmatrix} 0 \\ a_1 \end{pmatrix} = \begin{pmatrix} \epsilon_{01} & a_1 \\ \epsilon_{11} & a_1 \end{pmatrix}. \quad (19)$$

The nonzero first row of Eq. (19) means that the charge-exchange reaction in the model space can take place by a non-charge-exchange term in the effective interaction operator [see Eq. (15) for the definition of ϵ_{01}]. This feature is due to the assumed conservation of isospin of the total state, model plus core. The conservation requirement is brought about by the symmetry potential $V_{\mathrm{sym}} T^2$ which mixes the charge of the particle-hole excitation and the model space. Thus, because the charge of the model space and particle-hole space separately are not conserved, the operator producing the inelastic excitation and deexcitation need not transfer charge. The symmetry potential itself can transfer charge between model space and particle-hole space.

III. SCHEMATIC MODEL

In this section we derive a generalized schematic model of the isovector and isoscalar giant resonances with good isospin.[3] Although crude, this model contains the main features needed to show an example of the core-polarization effects we are developing. The schematic model with conservation of isospin has been treated for dipole states.[2] Here we treat the general electric multipole in the degenerate limit, which allows us to obtain explicit dependence on nuclear parameters. It is advantageous to start as in Eq. (4) with states of definite isospin. Here as in Ref. 1, we resort to the separable-potential model. We will need isospin uncoupled-uncoupled, coupled-uncoupled, and coupled-coupled matrix elements since our particle-hole states are both coupled (for matched particle-hole pairs) and uncoupled (for unmatched pairs) in isospin. The matrix elements needed are

$$\langle \lambda\mu(mi) | V | \lambda\mu(nj) \rangle = d_{mi} d_{nj} \begin{cases} V_0 + V_1 = \alpha, & \text{like ph pairs} \\ -V_0 + V_1 = -\beta, & \text{unlike ph pairs,} \end{cases} \quad (20a)$$

$$\langle \lambda\mu(mi) | V | \lambda\mu\tau 0(nj) \rangle = \sqrt{2}\, d_{mi} d_{nj} \begin{cases} V_1 & \tau = 1, \\ V_0 & \tau = 0, \ mi \text{ a proton ph pair}, \\ -V_0 & \tau = 0, \ mi \text{ a neutron ph pair}, \end{cases} \quad (20b)$$

and

$$\langle \lambda\mu\tau\rho(mi) | V | \lambda\mu\tau\rho(nj) \rangle = 2 d_{mi} d_{nj} (V_0 \delta_{\tau 0} + V_1 \delta_{\tau 1}), \quad (20c)$$

where

$$d_{mi} = \langle \lambda\mu(mi) | \mathcal{Q}_{\lambda\mu} | 0 \rangle = \frac{\langle j_m || Q_\lambda || j_i \rangle}{\hat{\lambda}} (-1)^{\lambda - j_m - j_i}. \quad (21)$$

These are obtained by calculating the exchange terms (particle-hole destruction plus creation) and dropping the direct terms (particle-hole scattering) in the particle-hole matrix element of the $\underline{Q}_\lambda \cdot \underline{Q}_\lambda$ interaction.

A. States with $T = T_0$

In this case the coefficients B and C of Eqs. (4a) can refer either to the isovector or isoscalar excitation. In fact, the solutions which occur are neither purely isoscalar or isovector. Inserting

Eq. (4a) into the Schrödinger equation and taking inner products of the resulting equations with single particle-hole excitations of each of the four types, unmatched neutron, unmatched proton, matched $\tau=0$, and matched $\tau=1$ gives a set of four coupled equations in the coefficients C^n_{mi}, C^p_{mi}, B^0_{mi}, and B^1_{mi}. In the interest of brevity, we record at this point only the first of these,

$$(E-\epsilon^0_{mi})C^n_{mi}=d_{mi}\Big(\alpha\sum_{m'i'}^{un}C^n_{m'i'}d_{m'i'}-\beta\sum_{m'i'}^{un}C^p_{m'i'}d_{m'i'} -\sqrt{2}\,V_0\sum_{m'i'}^{ma}B^0_{m'i'}d_{m'i'} +\sqrt{2}\,\rho V_1\sum_{m'i'}^{ma}B^1_{m'i'}d_{m'i'}\Big), \tag{22}$$

where the Clebsch-Gordan coefficient

$$\rho=\langle T_0 1 T_0 0\,|\,T_0 T_0\rangle=[T_0/(T_0+1)]^{1/2} \tag{23}$$

comes from the coupling to good isospin of particle-hole and model-space wave functions.

Taking the degenerate limit $\epsilon^0_{mi}=\epsilon^0=$ const, multiplying both sides of Eqs. (22) and the corresponding equations in the other coefficients by d_{mi} and summing over particle-hole pairs of a given kind gives four equations in a set of collective variables K_n, K_p, K_0, K_1, where, for example,

$$K_n=\sum_{mi}^{un}d_{mi}C^n_{mi}. \tag{24}$$

Transforming for convenience to new variables

$$\tilde{K}_0=\frac{-K_n+K_p}{\sqrt{2}}\,,\quad \tilde{K}_1=\frac{K_n+K_p}{\sqrt{2}}\,, \tag{25}$$

we can express these four equations as a matrix equation

$$\underline{M}\,\underline{K}=\underline{K}\,\Delta, \tag{26}$$

where

$$\underline{K}=(\tilde{K}_0 K_0 \tilde{K}_1 K_1)^T \tag{27}$$

and

$$\underline{M}=\begin{bmatrix} y^{un}_+V_0 & y^{un}_+V_0 & -y_-V_1 & -y_-V_1\rho \\ 2y^{ma}V_0 & 2y^{ma}V_0 & 0 & 0 \\ -y_-V_0 & -y_-V_0 & y^{un}_+V_1 & y^{un}_+V_1\rho \\ 0 & 0 & 2y^{ma}V_1\rho & 2y^{ma}V_1 \end{bmatrix}, \tag{28}$$

where

$$y_+=y^{un}_n+y^{un}_p+2y^{ma}=y^{un}_++2y^{ma} \tag{29}$$

and

$$y_-=y^{un}_n-y^{un}_p. \tag{30}$$

In Eqs. (29) and (30) y^{un}_n, y^{un}_p, and y^{ma} are, respectively, the sum of $d_{mi}{}^2$ over unmatched neutron, unmatched proton, and matched (neutron or proton) particle-hole pairs. The equations for $\tilde{K}_0$ and K_0 and those for $\tilde{K}_1$ and K_1 are nearly identical except for the y_- term. Since y_- is small compared to y_+, it is appropriate to treat the y_- terms as perturbations and carry them only to first order. When the y_- terms are dropped, the $\tilde{K}_0$ and K_0 equations are uncoupled from the $\tilde{K}_1$ and K_1 equations, so these pairs of equations can then be diagonalized separately. The details are carried out in Appendix A.

Before these solutions are presented, some remarks on the interpretation of $\tilde{K}_0$ and $\tilde{K}_1$ seem appropriate. The variables K_0 and K_1 are collective coordinates coming from linear combinations of particle-hole pairs of the matched type, which have definite isospin. On the other hand, $\tilde{K}_0$ and $\tilde{K}_1$ are linear combinations of neutron and proton terms in different particle-hole states and are, therefore,

TABLE I. The four solutions of the coupled equations for $T_<$ states.

n	State	$\tilde{K}_0/C_n$ [a]	K_0/C_n	$\tilde{K}_1/C_n$	K_1/C_n
0	Collective isoscalar	y^{un}_+	$2y^{ma}$	$\dfrac{-y_-(y_+V_0-2y^{ma}V_1)}{\beta y_+}$	$\dfrac{-2y^{ma}y_-V_1\rho}{\beta y_+}$
$\bar{0}$	Noncollective isoscalar	y^{un}_+	$-y^{un}_+$	0	0
1	Collective isovector	$\dfrac{y_-(y_+V_1\mp 2y^{ma}V_0)}{\beta y_+}$	$\dfrac{2y^{ma}y_-V_0}{\beta y_+}$	y^{un}_+	$\dfrac{2y^{ma}}{\rho}$
$\bar{1}$	Noncollective isovector	$\dfrac{-2y^{ma}y_-}{y_+}$	$\dfrac{2y^{ma}y_-}{y_+}$	y^{un}_+	$\dfrac{-y^{un}_+(y^{un}_+ +2y^{ma}\rho^2)}{\rho y_+}$

[a] To the same approximation as the table entries, one can show that

$C_0=C_{\bar{0}}=(2y_+)^{-1/2}$, $C_1=[2(y^{un}_+ +2y^{ma}/\rho)]^{-1/2}$,

and

$C_{\bar{1}}=[2y^{un}_+(1+y^{un}_+/2y^{ma}\rho^2)]^{-1/2}$.

totally mixed in isospin. Nevertheless, the collective solutions have either $\bar{K}_0+K_0$ large and $\bar{K}_1+K_1$ small or vice versa and behave with respect to transition operators as if they were nearly purely isoscalar or isovector. Thus these solutions in this rather crude nuclear model are precisely what Bohr and Mottelson[4] refer to as excitations which on the microscopic level are completely mixed in isospin, but which on a macroscopic level are fairly pure. The solutions obtained for $\bar{K}$ are given in Table I. The shift of the isoscalar and isovector states are approximately $V_0 y_+$ and $V_1 y_+$, respectively [see Eq. (A6)].

B. States with $T = T_0 + 1$

For these excitations we have the simple TDA function (4b) with $T = T_0+1$, and $T_z = T_0$. The Schrödinger equation gives

$$(E-\epsilon^0_{mi})B^1_{mi} = \sum_{m'i'}^{ma} 2V_1 B^1_{m'i'} d_{mi}\, d_{m'i'} \equiv 2V_1 d_{mi} K_1 . \tag{31a}$$

Multiplying by d_{mi}, summing and taking the degenerate limit $\epsilon^0_{mi} = \epsilon^0$ yields

$$\Delta K_1 = 2y^{ma} V_1 K_1 , \tag{31b}$$

giving an energy shift

$$\Delta \equiv E - \epsilon^0 = 2y^{ma} V_1 . \tag{32}$$

This is equivalent to Brown's[5] result, Ch. IV, Eq. (8.1), except that in this case only the matched particle-hole pairs are summed.

As the coefficients B^1_{mi} are proportional to d_{mi} as in Eq. (31), it must be true that

$$B^1_{mi}\ \frac{d_{mi}}{\left(\sum_{mi}^{ma} d_{mi}^2\right)^{1/2}} = \frac{d_{mi}}{(y^{ma})^{1/2}} \tag{33}$$

for normalization of the state. Then K_1 is

$$K_1 = \sum_{mi}^{ma} B^1_{mi} d_{mi} = \frac{\sum_{mi}^{ma} d_{mi}^2}{(y^{ma})^{1/2}} = (y^{ma})^{1/2} . \tag{34}$$

Having the wave function, we may now calculate the transition amplitudes, S^t_1, where t now refers to $T = T_0+1$ states. This is

$$\begin{aligned} S^t_1(\mathrm{ma}) &= \langle A^{1\dagger}_t \psi_{\mathrm{vac}} \,|\mathcal{O}_{IN1\rho}|\, \psi_{\mathrm{vac}} \rangle \\ &= \sqrt{2}\ \sum_{mi}^{ma} B^1_{mi} d_{mi} \\ &= (2y^{ma})^{1/2} . \end{aligned} \tag{35}$$

It is interesting to compare the shifts of the $T_<$ and $T_>$ isovector quadrupole state Eqs. (A6) and (32). Since $2y^{ma} < y_+$, Eq. (29), it is seen that the upward energy shift of the $T_>$ state is less than the shift of the $T_<$ state; however, the $T_>$ states are shifted up compared to the $T_<$ states by the Lane symmetry potential $\hat{V}_1$. The net shift (in MeV) is

$$\begin{aligned} \Delta E_T &= E_{T_0+1} - E_{T_0} \\ &= \frac{\hat{V}_1}{A}(T_0+1) - \Delta E_1 (1 - 2y^{ma}/y_+) \\ &= \frac{100}{A}(T_0+1) - \frac{38}{A^{1/3}}\left(\frac{a}{3} + \frac{6}{5a}\right)\xi , \end{aligned} \tag{36}$$

where the results for $2y^{ma}/y_+$ have been obtained by dividing Eq. (B6) multiplied by 2 by (B7a); a and ξ are given by Eqs. (B3) and (B4). In Eq. (36) the procedure of Ref. 1 is used whereby the amount of isovector particle-hole interaction strength is adjusted to fix the energy of the isovector collective state such that $\Delta E_1 = 120/A^{1/3} - 2\hbar\omega$. If the symmetry energy U_λ for quadrupole states is defined to include the particle-hole interactions in correspondence with what has been done[6] for dipole states, we obtain from Eq. (36)

$$\begin{aligned} U_2 &\equiv \frac{A}{T_0+1}\,\Delta E_T \\ &= 100 - 29(1 + 2.75/A^{2/3}) T_0/(T_0+1)\ \mathrm{MeV} . \end{aligned} \tag{37}$$

Because it is at best difficult to get an empirical determination of ΔE_T and, therefore, U_λ for the isovector quadrupole states, the results of our dipole-shift predictions compared to other work are included to support the credibility of our quadrupole estimates. Using the procedures of Appendix B for the dipole state, it can be shown that

$$\frac{2y^{ma}}{y_+} = 1 - \tfrac{2}{3}\,\xi a , \tag{38}$$

where the good isospin requirement $\omega_n = \omega_p$ has been used. This leads to a net shift for the dipole states given by

$$\Delta E_T = \frac{\hat{V}_1}{A}(T_0+1) - \left(\frac{80}{A^{1/3}} - \hbar\omega\right)\tfrac{2}{3}\,\xi a . \tag{39}$$

To the extent that the giant-dipole excitation matrix element is pure isovector, there is no correction for recoil needed in Eqs. (38) and (39). The correction due to impurity in the $T_<$ state is small and proportional to ξ^4 because the strength of the interaction and the impurity are each proportional to ξ. The dipole symmetry energy (in MeV) is then

$$U_1 = 100 - 60 T_0/(T_0+1). \tag{40}$$

If we had used $\langle r_n^2\rangle = \langle r_p^2\rangle$, the $\frac{2}{3}$ of Eq. (38) would be replaced by $\frac{1}{2}$. It follows that the second term of Eq. (40) would be 33% smaller so that U_1 would

then agree with the dipole symmetry energy of Ref. 6, $U_1 = 60$ MeV at $T_0 = 7$. For ^{90}Zr the symmetry energy from Eq. (40) is $U_1 = 50$ MeV. This result is lower than the 60 MeV of Ref. 6, but, because of the spread, both predictions are consistent with the data[7] for ^{90}Zr. In actual nuclei the results are probably somewhere between the extremes of taking $\langle r_n^2 \rangle = \langle r_p^2 \rangle$ and $\omega_n = \omega_p$. Indeed, the empirically determined average dipole symmetry energy is 55 ± 15 MeV,[7] which lies between these limits. In our good isospin schematic-model description, it would be inconsistent to take $\langle r_n^2 \rangle = \langle r_p^2 \rangle$, and, in any case, the present data do not require us to do so.

The ratio of the $T_>$ to $T_<$ particle-hole strengths, $2y^{ma}/y_+$, for the dipole and the quadrupole states is of interest in understanding their respective shifts. In both cases the relative amount of matched strength decreases with the neutron excess, but, since the quadrupole strength is made up of particle-hole excitations involving two major shells, the matched strength decreases more slowly. For the dipole state in ^{208}Pb our good isospin procedure ($\omega_n = \omega_p$) gives $2y^{ma}/y_+ = 0.051$, while for the quadrupole state the ratio is 0.484. These are intuitively pleasing results since we might guess these strengths to be zero and $\frac{1}{2}$, respectively, because in ^{208}Pb the dipole matched pairs are essentially blocked and the quadrupole matched pairs are nearly half blocked. (See also Sec. V B.) In contrast, for $\langle r_n^2 \rangle = \langle r_p^2 \rangle$, the dipole ratio $2y^{ma}/y_+ = 0.283$.

The net shift in energy of the giant isovector states is a result of the competition between the Lane symmetry term which dominates and which shifts states of higher isospin higher in energy and the particle-hole interaction which because of the smaller strength in the $T_>$ state, shifts the $T_<$ state higher in energy. Because $\Delta E_1 \approx 40/A^{1/3}$ is about the same for the dipole and quadrupole cases, and $2y^{ma}/y_+$ is considerably larger for the quadrupole state compared to the dipole state, the upward shift of the $T_>$ state compared to the $T_<$ state due to the particle-hole interaction is larger for the quadrupole states. Consequently, because the Lane symmetry term is equal and larger in magnitude than the particle-hole shifts for the two cases, the $T_>$ is higher in energy for both and the net shift is larger for the isovector quadrupole than dipole state.

IV. CALCULATION OF THE POLARIZATION PARAMETERS FOR ELECTRIC QUADRUPOLE TRANSITIONS

A. Calculation of transition amplitudes between $T = T_0$ states

From Eqs. (11) and (4a) using Eqs. (25), we obtain

$$S_\tau^t(\mathrm{un}) = \langle A_t^{\mathrm{un}\dagger} \psi_{\mathrm{vac}} \, | O_{\lambda\mu\tau 0} | \, \psi_{\mathrm{vac}} \rangle$$

$$= \left\langle \left(\sum_{mi}^{\mathrm{un}} C_{mi}^n a_{m\,1/2}^\dagger b_{i\,-1/2}^\dagger + \sum_{mi}^{\mathrm{un}} C_{mi}^p a_{m\,-1/2}^\dagger b_{i\,1/2}^\dagger \right) \psi_{\mathrm{vac}} \, | O_{\lambda\mu\tau 0} | \, \psi_{\mathrm{vac}} \right\rangle$$

$$= \sum_{mi}^{\mathrm{un}} C_{mi}^n d_{mi} - (-1)^\tau \sum_{mi}^{\mathrm{un}} C_{mi}^P d_{mi} = K_n - (-1)^\tau K_p = (-1)^{\tau+1} \sqrt{2}\, \tilde{K}_\tau , \tag{41}$$

and

$$S_\tau^t(\mathrm{ma}) = \langle A_t^{\tau\dagger} \psi_{\mathrm{vac}} \, | O_{\lambda\mu\tau 0} | \, \psi_{\mathrm{vac}} \rangle = (-1)^{\tau+1} \sqrt{2} \sum_{mi}^{\mathrm{ma}} B_{mi}^\tau d_{mi} = (-1)^{\tau+1} \sqrt{2}\, K_\tau . \tag{42}$$

Thus the transition amplitudes Eqs. (11) are simply proportional to the appropriate $\tilde{K}_\tau$ or K_τ from Table I.

The elements of the polarization matrix can now be calculated from Eq. (15). The results are

$$\epsilon_{00} = 1 - 2\,\frac{\Delta E_0}{E_0} = 1.74 ,$$

$$\epsilon_{11} \approx 1 - \frac{2\Delta E_1}{E_1} = 0.366 ,$$

$$\epsilon_{10} = \frac{V_1}{V_0 - V_1}\,\frac{y_-}{y_+}\,(\epsilon_{00} - \epsilon_{11}) ,$$

$$\epsilon_{01} = \frac{V_0}{V_1}\,\epsilon_{10} + \frac{2y^{ma} y_- V_0}{(V_0 - V_1) y_+^2 (T_0 + 1)} \times \left(\frac{-V_1}{V_0}\,\epsilon_{00}^{\mathrm{pol}} + \epsilon_{11}^{\mathrm{pol}} \right) , \tag{43}$$

where the amount of polarizing interaction strength V_τ in Eq. (15) has been adjusted to fix the energies

TABLE II. Polarization parameters for $T_<$ quadrupole transitions with corrections for good isospin. The no-parameter schematic model (NPSM) is used with $\omega_n = \omega_p$.

Nucleus	ϵ_{10}	ϵ_{01} [a]	ϵ_{01} [b]	(β_1/β_0) [a]	(β_1/β_0) [b]
^{44}Ca	−0.055	0.110	0.104	3.11	3.09
^{90}Zr	−0.067	0.136	0.131	−1.15	−1.18
^{118}Sn	−0.093	0.186	0.182	2.18	2.19
^{207}Pb	−0.125	0.255	0.249	1.83	1.84

[a] Calculated from formulas of Ref. 1.
[b] Corrected for good isospin.

of the isoscalar and isovector ($T_<$) collective states at $60/A^{1/3}$ and $120/A^{1/3}$, respectively. The expressions in Eq. (43) are all the same as in the no-parameter schematic model (NPSM) of Ref. 1, where no account was taken of isospin conservation, except for ϵ_{01} in which the second term is a correction which is small for large neutron-excess nuclei (see Sec. II A).

In Table II the polarization parameters for quadrupole $T_0 \to T_0$ transitions are presented for some typical nuclei along with values of the isovector to isoscalar deformation parameters[8] β_1/β_0. The parameters ϵ_{10} are double those of the NPSM of Ref. 1 due to the use of $\omega_n = \omega_p$ for the harmonic oscillators instead of $\langle r_n^2\rangle = \langle r_p^2\rangle$. The former relation was chosen because it is necessary for good isospin single-particle states. The correction for good isospin is seen to make only small differences for ϵ_{01} and β_1/β_0. The largest changes occur for small T_0 for reasons stated in Sec. II A. In contrast the effect of using $\omega_n = \omega_p$ as opposed to $\langle r_n^2\rangle = \langle r_p^2\rangle$ as described above makes sizable changes in the ϵ's. On the other hand, the inelastic β ratios such as $\beta_{\alpha\alpha'}/\beta_{\rm em}$ are much less sensitive to these model assumptions.

Polarization parameters for charge exchange to 2^+ excited-analog states are the same as those that enter in the isovector part of the inelastic scattering to the parent 2^+ state because of our imposition of definite isospin on the wave functions of Eq. (5). For low-lying collective 2^+ states the quantities of interest are the isovector and isoscalar deformation parameters β_1 and β_0. The β_1/β_0 ratios predicted by our core-polarization model, including the small changes for good isospin, are quite different, even including a sign change, for proton-valence nuclei and neutron-valence nuclei as seen in Table II. Direct empirical determination of the isovector deformation parameter β_1 is difficult because the (p,n) excited-analog transition takes place primarily by two-step processes involving isoscalar and isovector transitions, and, furthermore, the one- and two-step processes are nearly incoherent.[9] Other projectiles such as ^{3}He and pions should have an advantage because the first-order interaction has a nonreal phase which would be expected to lead to more interference between the one- and two-step processes. Lacking direct empirical evidence, indirect evidence, which comes about because of the differences in the isovector deformation parameters corresponding to various external fields, can be obtained from inelastic scattering and electromagnetic transitions. Recent studies[8,10,11] comparing (n,n'), (p,p'), (α,α'), and electromagnetic transitions are consistent with our predictions.

B. Transition amplitudes between T_0 and $T_0 + 1$ states

For this case ϵ is one dimensional and is given trivially by Eq. (18) as

$$\epsilon = 1 - \frac{2V_1}{E_t}\,|S_1^t(\mathrm{ma})|^2 = 1 - \frac{2V_1}{E_t}\,(2y^{\mathrm{ma}}). \tag{44}$$

V. TRANSITIONS TO GIANT STATES

In this section we use the values of the transition matrix elements S_τ^t to estimate multipole-transition rates for various giant resonances.

A. Inelastic scattering to the $T_<$ state

For the isoscalar state one has

$$|S_0^0|^2 = y_+ = \frac{5}{16\pi}\left(\frac{\hbar}{\mu\omega}\right)^2\left(\frac{3A}{2}\right)^{4/3} \tag{45}$$

and

$$\left|\frac{S_1^0}{S_0^0}\right|^2 = (\tfrac{4}{3}\xi)^2\left(\frac{V_0}{V_0 - V_1}\right)^2\left(1 - \frac{2y^{\mathrm{ma}}}{y_+}\,\frac{V_1}{V_0}\,\frac{1}{T_0+1}\right)^2. \tag{46}$$

The factor in front $\frac{4}{3}\xi$ is due to the assumption that $\omega_n = \omega_p$. For $\langle r_n^2\rangle = \langle r_p^2\rangle$ it is $\frac{2}{3}\xi$, and in reality it is probably somewhere in between. In RPA $|S_0^0|$ is increased by a factor of ϵ^0/E, but the ratio is maintained. For ^{208}Pb the ratio is about 4%, which means that the cross section for exciting the isoscalar giant resonance with a pure isovector field, such as in (p,n) is small.

For the isovector state

$$|S_1^1|^2 = \left|y_+\Big/\left(y_+^{\mathrm{un}} + 2y^{\mathrm{ma}}\,\frac{T_0+1}{T_0}\right)^{1/2}\right|^2 \approx y_+, \tag{47}$$

and

$$\left|\frac{S_0^1}{S_1^1}\right|^2 = (\tfrac{4}{3}\xi)^2\left(\frac{V_1}{V_0 - V_1}\right)^2. \tag{48}$$

Again, in RPA S_1^1 is reduced by a factor ϵ^0/E, but the ratio Eq. (48) is maintained (~1% for ^{208}Pb).

B. Excitation of $T = T_0 + 1$ states

The multipole matrix element for exciting the giant state $T = T_0 + 1$ [used in obtaining Eq. (18)] is given by

$$\langle [A_t^{1\dagger}\psi_t^0]_f | \mathcal{O}_{\lambda\mu 1\rho} | \psi_i^0 \rangle = \langle J_i \lambda M_i \mu | J_f M_f \rangle \langle T_0 1 T\rho | T T_z \rangle S_1^t(\mathrm{ma}). \quad (49)$$

The isospin Clebsch-Gordan coefficient for $T = T_0 + 1$ states is near 1 for $T_z = T_0 + 1 \gg 1$ and small for $T_z = T_0$. Thus the (n,p) reaction to the $T_>$ giant resonance should be large, the (p,p') small, and the (p,n) yet smaller for large T_0.

As an example, we estimate the ratio of the ^{208}Pb(p,p') cross section for the $T_>$ state to that for the isoscalar state. Using Eqs. (12) and (45) for the isoscalar transition and Eqs. (49) and (35) for the $T_>$ transition with the appropriate projectile isospin Clebsch-Gordan coefficients, the cross-section ratio becomes

$$\frac{\sigma_{T_>}(p,p')}{\sigma_{\text{isoscalar}}(p,p')} \approx \left(\frac{V_1}{V_0}\right)^2 \frac{2y^{\mathrm{ma}}}{y_+} \langle T_0 1 T_0 0 | T T_0 \rangle^2 \langle \tfrac{1}{2} 1, -\tfrac{1}{2} 0 | \tfrac{1}{2}, -\tfrac{1}{2} \rangle^2 = \left(\frac{V_1}{V_0}\right)^2 \frac{2y^{\mathrm{ma}}}{y_+} \frac{1}{T_0+1} \tfrac{1}{3}. \quad (50)$$

For $E1$ transitions y^{ma} is essentially zero for Pb due to blocking of matched pairs, so there is no $T_>$ transition, but as $E2$ involves $2\hbar\omega$ transitions there is only partial blocking, and the ratio $2y^{\mathrm{ma}}/y_+$ of matched pairs to total pairs can be obtained as in Eq. (36). For nuclei with a small neutron excess, $2y^{\mathrm{ma}}/y_+$ is near 1; almost all pairs are matched. For ^{208}Pb it is $\approx \frac{1}{2}$. (See Sec. III B.) The Clebsch-Gordan coefficient, however, is very unfavorable, and the expected ratio Eq. (50) using $V_1/V_0 \approx -\frac{1}{2}$ is 0.0018. On the other hand, the ratio of the (n,p) transition to the T_0+1 parent-analog state with the appropriate isospin Clebsch-Gordan coefficients should be

$$\frac{\sigma_{T_>}(n,p)}{\sigma_{\text{isoscalar}}(p,p')} = \left(\frac{\sqrt{2}\,V_1}{V_0}\right)^2 \frac{2y^{\mathrm{ma}}}{y_+} \approx 0.242. \quad (51)$$

From the known ^{208}Pb(p,p') cross section[12] for the $E2$ isoscalar state of about 6.5 mb/sr at 15° we get a ^{208}Pb(n,p) cross section of 1.6 mb/sr. However, because of the high energy of the $T_>$ quadrupole state, it is expected[13] to be spread considerably and will probably not be visible as a sharp resonance.

VI. SUMMARY AND DISCUSSION

We have shown that the $\underline{\epsilon}$ matrix relating core polarization in inelastic scattering and electromagnetic transitions can also be applied in charge-exchange reaction. The schematic model is used to show that the correction to the $\underline{\epsilon}$ matrix from the imposition of isospin conservation is small. The ratio of isovector to isoscalar deformation parameters β_1/β_0 is calculated for typical single-closed-shell nuclei, and the correction is likewise small. The β_1 parameter applies not only to inelastic scattering but also charge exchange under the assumption of isospin conservation.

It should be pointed out, however, that, although isospin splitting is expected for giant resonance states, the purity need not be very great. In contrast, the impurity in a low lying nuclear state resulting from mixing with this giant state as in Eq. (5) will be small. It is not likely that this impurity will result in much change in the $\underline{\epsilon}$ matrix. On the other hand, it may affect the validity of the simple connection between inelastic scattering and charge exchange and, therefore, decrease the accuracy of Eq. (19) for the charge-exchange amplitudes.

Keeping in mind the above and other obvious limitations due to the rudimental nature of the model, we can ask what the present data tell us about the qualitative, if not quantitative, correctness of our ideas. Unfortunately, there is at present no direct determination of the isovector transition strength. This effect is masked in (p,n) excited-analog transitions to low lying 2^+ states because of the dominance of the two-step and the relative phase of the one- and two-step mechanisms.[9] The indirect evidence,[8,10,11] involving a comparison between external fields such as (p,p'), (n,n'), (α,α'), and electromagnetic transitions, is consistent with our predictions for β_1/β_0. (The correction for good isospin does not alter these earlier conclusions.) In the usual collective model with equal β's, the isovector part of the multipole transition operator used for inelastic scattering and electromagnetic transitions is of the order of 7% which makes the difference for (p,p') and (n,n') of the order of 14%. Our shell effects moderated by core polarization produce fluctuations in the isovector to isoscalar ratio of the same order. It is at this level, then, that our isospin effects are corroborated by the inelastic and electromagnetic data. Continued effort in the direction of indirect confirmation as well as further investigation of the possibility of a direct determination of β_1/β_0 such as by pion charge exchange or $(^3\mathrm{He},t)$ is necessary before a clear separation of the isoscalar and isovector ef-

fects can be made.

Results of the schematic model are used to estimate the energy splitting between the quadrupole-isovector $T_>$ and $T_<$ states. Comparison of our corresponding predictions on dipole splitting to earlier work,[6,7] done in the same spirit, gives us confidence to apply our results to the quadrupole case, where measurements are not available. Our dipole results differ from the earlier ones in that they depend on mass number and neutron excess, but neither this dependence nor the difference in the size of the effect compared to the earlier work is ruled out by the data. The net shift in energy of the giant quadrupole isovector states is predicted by our calculations to be larger than that for the dipole states. This is because the $T_>$ quadrupole strength suffers less from blocking effects since it involves transitions from two major shells below the Fermi sea.

Determination of the core-polarization matrix requires calculation of the multipole transition strength for isoscalar and isovector multipole resonances. These results are applied to estimating some cross sections for directly exciting giant $E2$ states. Cross section ratios of the giant quadrupole $T_>$ (p,p') and (n,p) to the corresponding isoscalar (p,p') are determined from our model. The known[12] ^{208}Pb(p,p') giant $E2$ isoscalar cross section is then used to predict the other two. Because of the unfavorable isospin Clebsch-Gordan coefficient, the $T_>(p,p')$ cross section is extremely small, but the (n,p) cross section of the parent analog of the giant quadrupole $T_>$ in ^{208}Pb at 15° is predicted to be ~1.6 mb/sr. Both for this (n,p) transition and the above discussion of the isovector splitting one should keep in mind that on the basis of more realistic RPA calculations,[13] the giant isovector $T_>$ is expected to be spread considerably, thereby making empirical determinations of these effects at best difficult.

APPENDIX A. SOLUTION OF COUPLED EQUATIONS FOR $T_<$ STATES

Here we describe briefly the method of solution of Eq. (26). The first step is to diagonalize the matrix $\underline{M}$, Eq. (28) with the y_- elements set to zero. To this end we write Eq. (28) as

$$\underline{M}=\begin{bmatrix}\underline{m}_{00} & \underline{m}_{01}\\ \underline{m}_{10} & \underline{m}_{11}\end{bmatrix}, \tag{A1}$$

where the $\underline{m}_{ij}$ are 2×2 submatrices. We first then diagonalize a reduced $\underline{M}$ matrix in which $\underline{m}_{01}=\underline{m}_{10}=0$, which leaves two uncoupled eigenvalue problems. The four solutions for this subproblem are the collective (0) and noncollective $(\bar{0})$ isoscalar and the collective (1) and noncollective $(\bar{1})$ isovector. The presence of the $\underline{m}_{01}$ and $\underline{m}_{10}$ terms, proportional to y_- and therefore to neutron excess, mixes the two collective solutions giving rise to giant resonances which are nearly purely isoscalar or isovector but have a small component of the opposite type.

Let $\underline{X}^{-1}$ be the transformation matrix to the representation in which the reduced M matrix is diagonal. Equation (26) can be transformed to

$$\underline{M}'\underline{K}'=\underline{X}^{-1}\underline{M}\underline{X}\underline{X}^{-1}\underline{K}=\underline{X}^{-1}\underline{K}\underline{\Delta}=\underline{K}'\underline{\Delta}, \tag{A2}$$

the only off-diagonal elements of $\underline{X}^{-1}\underline{M}\underline{X}\equiv\underline{M}'$ being proportional to y_-, and these can now be treated using a perturbation expansion. We can see immediately that the eigenvalues are unchanged to first order in y_- by the presence of the nonzero off-diagonal matrices $\underline{m}_{01}$ and $\underline{m}_{10}$, since the first order corrections to the eigenvalues in perturbation theory are the diagonal elements of the perturbation, which are zero. The eigenvector $\underline{K}'=\underline{X}^{-1}\underline{K}$ can then be written

$$\underline{K}'_n=\underline{K}'^{(0)}_n+\underline{K}'^{(1)}_n, \tag{A3}$$

where $\underline{K}'^{(0)}_n$ is the nth exact solution of the subproblem. $\underline{K}'^{(1)}_n$ can be expanded in terms of the other three zero-order solutions,

$$\underline{K}'^{(1)}_n=\sum_{n'\neq n}\underline{K}'^{(0)}_{n'}\underline{a}_{n'n}, \tag{A4}$$

and substituted into Eq. (A3), which to first order in y_- is

$$\underline{K}'_n=C_n\left[\begin{pmatrix}\delta_{n0}\\ \delta_{n\bar{0}}\\ \delta_{n1}\\ \delta_{n\bar{1}}\end{pmatrix}-\sum_{n'\neq n}\frac{1}{\Delta_{n'}-\Delta_n}\begin{pmatrix}0 & \underline{m}'_{01}\\ \underline{m}'_{10} & 0\end{pmatrix}\right], \tag{A5}$$

where

$$\Delta_0=V_0y_+,\quad \Delta_{\bar{0}}=0,\quad \Delta_1=V_1(y_+-\delta),\quad \text{and } \Delta_{\bar{1}}=V_1\delta \tag{A6}$$

are the energy shifts for the four states, and

$$\delta=\tfrac{1}{2}y_+-\tfrac{1}{2}[y_+^2-2y^{ma}y^{un}_+(1-\rho^2)]^{1/2}$$

$$\approx\frac{2y^{ma}y^{un}_+(1-\rho^2)}{y_+}. \tag{A7}$$

The transformation matrices $\underline{X}$ from $\underline{K}'$ to $\underline{K}$ are composed of four column eigenvectors of the reduced eigenvalue problem. They can be applied to transform the solutions (A5) of the complete eigenvalue problem to give the eigenvectors $\underline{K}$, the elements of which are given in Table I. In this table terms of order δ are dropped unless they appear linearly with other small terms.

APPENDIX B. QUADRUPOLE SUM RULES FOR MATCHED AND UNMATCHED PAIRS

In Fig. 1 it is seen that, roughly speaking, the strength parameter for unmatched neutrons comes from the neutron excess. (This would be rigorously true for a harmonic-oscillator double-closed-shell nucleus without spin-orbit coupling.) The middle line of Eq. (B6) of Ref. 1 gives[14] the summed-squared quadrupole transition strength. The lower limit on the sum is taken to be zero to get a running sum from zero to η, with the result for the η' sum

$$\sum_{\eta'=0}^{\eta}(\eta'+1)(\eta'+2)(\eta'+3)(\eta'+4)=\frac{(\eta+1)(\eta+2)(\eta+3)(\eta+4)(\eta+5)}{5}\,. \tag{B1}$$

The parameter η is now allowed to be continuous and related to the total number of particles through Eq. (B8) of Ref. 1, and the unmatched neutron quadrupole strength $y_n^{\rm un}$ is now

$$\begin{aligned} y_n^{\rm un}=y(N)-y(Z)&\approx\frac{3}{64\pi}\left(\frac{\hbar}{\mu\omega}\right)^2[N((3N)^{1/3}+2)((3N)^{1/3}+3)-Z((3Z)^{1/3}+2)((3Z)^{1/3}+3)]\\ &\approx\frac{1}{64\pi}\left(\frac{\hbar}{\mu\omega}\right)^2 A\xi(5a^2+20a+18)\,, \end{aligned} \tag{B2}$$

where the good approximation $(\eta+2)=(3N)^{1/3}$ has been used,

$$a=\left(\frac{3A}{2}\right)^{1/3} \tag{B3}$$

and

$$\xi=\frac{N-Z}{A}\,. \tag{B4}$$

The total neutron strength is obtained from Eq. (B6) of Ref. 1 and is given by

$$y_n\approx\frac{5}{32\pi}\left(\frac{\hbar}{\mu\omega}\right)^2(3N)^{4/3}=\frac{1}{64\pi}\left(\frac{\hbar}{\mu\omega}\right)^2 Aa(15+20\xi)\,. \tag{B5}$$

Then the matched strength is

$$y^{\rm ma}=y_n-y_n^{\rm un}\approx\frac{1}{64\pi}\left(\frac{\hbar}{\mu\omega}\right)^2 A[15a-(15a^2+18)\xi]\,, \tag{B6}$$

and the sum and difference strengths are

$$\begin{aligned} y_\pm&\approx\frac{5}{32\pi}\left(\frac{\hbar}{\mu\omega}\right)^2[(3N)^{4/3}\pm(3Z)^{4/3}]\\ &\approx\frac{5}{32\pi}\left(\frac{\hbar}{\mu\omega}\right)^2\left(\frac{3A}{2}\right)^{4/3}[(1+\tfrac{4}{3}\xi)\pm(1-\tfrac{4}{3}\xi)]\\ &=\frac{5}{16\pi}\left(\frac{\hbar}{\mu\omega}\right)^2 a^4\begin{cases}1 & \text{(B7a)}\\ \tfrac{4}{3}\xi & \text{(B7b)}\end{cases}. \end{aligned}$$

Then we can obtain

$$y_+^{\rm un}=y_+-2y^{\rm ma}=\frac{1}{32\pi}\left(\frac{\hbar}{\mu\omega}\right)^2 A(5a^2+18)\xi\,. \tag{B8}$$

For the double-closed-shell harmonic-oscillator nucleus $N=112$, $Z=70$, these approximations are within 1% except for $y_+^{\rm ma}$ which is 3% low. For ^{48}Ca an exact calculation with explicit summing was made of $y_+^{\rm ma}$, giving 33 in units of $(\hbar/\mu\omega)^2\pi^{-1}$ compared with Eq. (B6) which gives 33.7. The same calculation gave a value of $y_\flat$ which is 4.5 compared to the value calculated using the same approximations as in Eqs. (B5)–(B7) of 3.8. This difference will not matter much since $y_\flat$ is itself rather small and unimportant in this case.

*This work was performed under the auspices of the U. S. Energy Research and Development Administration under contract No. W-7405-Eng-48.

†This work was performed in part as a Lawrence Livermore Laboratory summer visitor in 1976 and in part at the Institute für Kernphysik, D517 Jülich, West Germany.

[1]V. R. Brown and V. A. Madsen, Phys. Rev. C 11, 1298 (1975).

[2]B. Goulard, T. A. Hughes, and S. Fallieros, Phys. Rev. 176, 1345 (1968); A. Jaffrin and G. Ripka, Nucl. Phys. A119, 529 (1968).

[3]It is important to distinguish between the isospin of the excitation and that of the nucleus. Three different types of isospin purity actually arise: the microscopic isospin of the giant resonance, the macroscopic isospin of the giant resonance as manifested by transition amplitudes, and the isospin of the nucleus as a whole in a giant excitation. As discussed in Sec. III, the first of these is very impure, the second is rather pure, and the third can still be totally pure as assumed in this paper.

[4]A. Bohr and B. R. Mottelson, *Nuclear Structure* (Benjamin, New York, 1975), Vol. II, Chap. 6.
[5]G. E. Brown, *Unified Theory of Nuclear Models and Forces* (North-Holland, Amsterdam, 1971), p. 29.
[6]R. Ö. Akyüz and S. Fallieros, Phys. Rev. Lett. 27, 1016 (1971).
[7]P. Paul, in *Proceedings of the International Conference on Photonuclear Reactions and Applications*, Asilomar, 1973, edited by B. L. Berman (U.S. Atomic Energy Commission, Asilomar, 1973), Vol. 1, p. 407.
[8]V. A. Madsen, V. R. Brown, and J. D. Anderson, Phys. Rev. C 12, 1205 (1975).
[9]V. A. Madsen, M. J. Stomp, V. R. Brown, J. D. Anderson, L. F. Hansen, C. Wong, and J. J. Wesolowski, Phys. Rev. Lett. 28, 629 (1972).
[10]D. E. Bainum, R. W. Finlay, J. Rapaport, J. D. Carlson, and J. R. Comfort, Phys. Rev. Lett. 39, 443 (1977).
[11]A. M. Bernstein, V. R. Brown, and V. A. Madsen, Phys. Lett. 71B, 48 (1977).
[12]F. Bertrand, Annu. Rev. Nucl. Sci. 26, 457 (1976).
[13]J. Speth and J. Wambach, private communication.
[14]Although the result Eq. (B6) of Ref. 1 is correct, the summand in the second line is incorrect and should read $\frac{1}{6}(\eta'+1)(\eta'+2)(\eta'+3)(\eta'+4)$. The corrected summand is treated in Eq. (B1) above.